Ferromagnetic-insulators-modulated transport properties on the surface of a topological insulator*

Guo Jun-Ji(郭俊吉) and Liao Wen-Hu (廖文虎)†

College of Physics, Mechanical and Electrical Engineering, Jishou University, Jishou 416000, *China*

(Received 11 September 2013; revised manuscript received 24 January 2014; published online 20 April 2014)

Transport properties on the surface of a topological insulator (TI) under the modulation of a two-dimensional (2D) ferromagnet/ferromagnet junction are investigated by the method of wave function matching. The single ferromagnetic barrier modulated transmission probability is expected to be a periodic function of the polarization angle and the planar rotation angle, that decreases with the strength of the magnetic proximity exchange increasing. However, the transmission probability for the double ferromagnetic insulators modulated n–n junction and n–p junction is not a periodic function of polarization angle nor planar rotation angle, owing to the combined effects of the double ferromagnetic insulators and the barrier potential. Since the energy gap between the conduction band and the valence band is narrowed and widened respectively in ranges of $0 \leq \theta < \pi/2$ and $\pi/2 < \theta \leq \pi$, the transmission probability of the n–n junction first increases rapidly and then decreases slowly with the increase of the magnetic proximity exchange strength. While the transmission probability for the n–p junction demonstrates an opposite trend on the strength of the magnetic proximity exchange because the band gaps contrarily vary. The obtained results may lead to the possible realization of a magnetic/electric switch based on TIs and be useful in further understanding the surface states of TIs.

Keywords: transport properties, surface state Dirac electron, topological insulator, ferromagnetic insulators

PACS: 71.10.Pm, 72.25.Dc, 73.20.–r **DOI:** 10.1088/1674-1056/23/6/067104

Topological insulators (TIs) have attracted increasing attention[1–8] due to the possibility of unveiling peculiar spin and charge transport phenomena.[9–12] The combined spin–orbit interaction[13] and reversal symmetry[14–16] have produced profound effects on physical properties of TIs, while the ferromagnetic insulators-induced time-reversal symmetry breaking[17–19] offers even richer properties of TIs.[20–28]

The magnetoresistance effect,[20–22] spin Hall effect,[23] charge current[24] other than the electrically controlled magnetization[25] in ferromagnet/TI heterostructures have been investigated. The Klein tunneling may be manipulated or even turned off by ferromagnetic barriers,[26] while the influences of magnetization[27] and width[28] of the ferromagnetic strip on transport properties of TIs and relevant materials[29–37] have been demonstrated, respectively. Furthermore, the proximity-induced ferromagnetism and superconductivity,[38] magnetization precession-induced charge pumping effect[39] including an electric switch[40] based on TIs have been predicted. Very recently, Zhai and Mu[41] investigated the transport features of Dirac electrons on the surface of a TI under the modulation of periodic ferromagnetic insulating stripes,[42] except for the electrically charged domain walls and vortices[43] in the ferromagnetic thin film deposited on the surface of a TI. The adiabatic quantum pumping[44] of Dirac fermions on the surface of a TI under the modulation of ferromagnets[45–49] has been demonstrated too.

Nevertheless, the influences of the ferromagnetic proximity exchange strength and the gate voltage-tuned barrier strength on the transmission probability of the Dirac electrons on the surface of TIs have not been discussed in previous literature,[20–28,38–49] but we address this important issue in the present work. Owing to the variations of the Fermi-surface and the wave function matching conditions,[26] the double ferromagnetic insulators-modulated transmission probabilities for the n–n junction and the n–p junction are qualitatively and quantitatively different from those under the modulation of the single ferromagnetic barrier, though all of them are sensitively dependent on the strength and orientation of the magnetic proximity exchange. The observed results may be useful in further understanding the surface states[50–52] of TIs and in magnetic/electric applications based on TIs.[40]

As illustrated in Fig. 1, the system is composed of two-dimensional (2D) ferromagnet/ferromagnet insulators deposited on the surface of a strong three-dimensional (3D) TI, with the ferromagnetic proximity exchange field $\boldsymbol{m}_1 = (m_x, m_y, m_z) \equiv m_1(\sin\theta\cos\varphi, \sin\theta\sin\varphi, \cos\theta)$ polarized along the arbitrary orientations while $\boldsymbol{m}_2 = m_2(0,0,1)$ in the z direction, and the surface current flows along the x direction. Taking into account a large enough mean-free path and phase coherence length, restricting the theoretical conditions at the weak disorder, and affecting the 2D Dirac electron mainly by the magnetic field of the ferromagnetic insulators

*Project supported by the National Natural Science Foundation of China (Grant Nos. 11264013 and 11147021), the Hunan Provincial Natural Science Foundation of China (Grant No. 12JJ4003), and the Research Program for Employee of Jishou University, China (Grant No. jsdxkyzz201005).

†Corresponding author. E-mail: whliao2007@aliyun.com

© 2014 Chinese Physical Society and IOP Publishing Ltd

rather than its stray field,[26] we obtain the system Hamiltonian as follows:

$$H = \hbar v_{\mathrm{F}} \boldsymbol{k} \cdot \boldsymbol{\sigma} + \boldsymbol{m} \cdot \boldsymbol{\sigma}, \tag{1}$$

where the Fermi velocity v_{F} and $\hbar$ are usually set to be 1 in the nondimensionalized process, and $\boldsymbol{\sigma} = (\sigma_x, \sigma_y, \sigma_z)$ denotes the spin of the surface state electrons.[19] Owing to the translation symmetry along the transversal direction, one can neglect the $\mathrm{e}^{\mathrm{i}k_y y}$ in the following for simplicity. The wave function in the range of $x \leq 0$ is

$$\begin{aligned}&\psi(x \leq 0)\\ &= \frac{\mathrm{e}^{\mathrm{i}k_x x}}{[2E(E-m_z)]^{1/2}} \begin{pmatrix} k_x + m_x - \mathrm{i}(k_y + m_y) \\ E - m_z \end{pmatrix}\\ &\quad + \frac{r\mathrm{e}^{-\mathrm{i}k_x x}}{[2E(E-m_z)]^{1/2}} \begin{pmatrix} -k_x - m_x - \mathrm{i}(k_y + m_y) \\ E - m_z \end{pmatrix}, \end{aligned} \tag{2}$$

where r is the reflection amplitude and the corresponding dispersion relation is $E = [(m_x + k_x)^2 + (m_y + k_y)^2 + m_z^2]^{1/2}$.

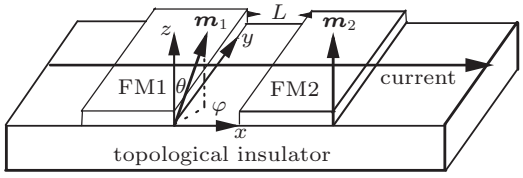


Fig. 1. Ferromagnetic proximity exchange field $\boldsymbol{m}_1 = (m_x, m_y, m_z) \equiv m_1$ $(\sin\theta\cos\varphi,\ \sin\theta\sin\varphi,\ \cos\theta)$ polarized along the arbitrary directions and $\boldsymbol{m}_2 = m_2(0,0,1)$ in the z direction, and the surface current flows along the x direction of the topological insulator.

On the assumption that the depletion layer, owing to the mismatch effect of the wave functions and the size of the Fermi surface, is narrow enough, meeting the conditions of the thin barrier limit for which $U \to \infty$ and $L \to 0$, while keeping the dimensionless barrier strength $Z = UL$ finite,[26–39] the wave function in the depletion layer $0 \leq x \leq L$ reads

$$\begin{aligned}&\psi(0 \leq x \leq L)\\ &= a\mathrm{e}^{\mathrm{i}k''_x x} \begin{pmatrix} k''_x - \mathrm{i}k_y \\ E - U \end{pmatrix} + b\mathrm{e}^{-\mathrm{i}k''_x x} \begin{pmatrix} -k''_x - \mathrm{i}k_y \\ E - U \end{pmatrix}, \end{aligned} \tag{3}$$

where the corresponding dispersion relation is $E = U - (k_y^2 + k_x''^2)^{1/2}$ with a (b) being the amplitude of right (left) moving electrons in the depletion region. Due to the built-in electric field contained in the interface of the ferromagnet/ferromagnet junction, naturally a potential drop V (can be tuned by the gate electrode) should be taken into account in the regime of $x \geq L$, therefore, the wave function takes the form of

$$\psi(x \geq L) = \frac{t\mathrm{e}^{\mathrm{i}k'_x x}}{[2E'(E'-m_2)]^{1/2}} \begin{pmatrix} k'_x - \mathrm{i}k_y \\ E' - m_2 \end{pmatrix}, \tag{4}$$

where t is the transmission amplitude and the dispersion relation $E' = E - V = \pm(k_x'^2 + k_y^2 + m_2^2)^{1/2}$ with $\pm$ denoting the conduction and valence bands, respectively. Matching boundary conditions between FM1 and the depletion layer at $x = 0$ and between the depletion layer and FM2 at $x = L$, we have

$$\frac{(1-r)(k_x + m_x) - \mathrm{i}(1+r)(k_y + m_y)}{[2E(E-m_z)]^{1/2}[a(k''_x - \mathrm{i}k_y) - b(k''_x + \mathrm{i}k_y)]} = 1, \tag{5}$$

$$\frac{(E-m_z)(1+r)}{[2E(E-m_z)]^{1/2}(a+b)(E-U)} = 1, \tag{6}$$

$$\frac{t(k'_x - \mathrm{i}k_y)\mathrm{e}^{\mathrm{i}k'_x L}}{[2E'(E'-V)]^{1/2}[a(k''_x - \mathrm{i}k_y)\mathrm{e}^{\mathrm{i}k''_x L} - b(k''_x + \mathrm{i}k_y)\mathrm{e}^{-\mathrm{i}k''_x L}]} = 1, \tag{7}$$

$$\frac{t\mathrm{e}^{\mathrm{i}k'_x L}(E'-m_2)^{1/2}}{(2E')^{1/2}(E-U)[a\mathrm{e}^{\mathrm{i}k''_x L} + b\mathrm{e}^{-\mathrm{i}k''_x L}]} = 1. \tag{8}$$

After some algebra from Eqs. (5)–(8), one obtains the system transmission amplitude

$$t = (A+B)/(C+D), \tag{9}$$

with

$$\begin{aligned} A &= 2[E^{-1}E'(E'-m_2)(E-m_z)\\ &\quad \times (E^2 - m_y^2 - m_z^2)]^{1/2}\sec Z, \end{aligned} \tag{10}$$

$$\begin{aligned} B &= 2\mathrm{i}[E^{-1}E'(E'-m_2)(E-m_z)\\ &\quad \times (E^2 - m_y^2 - m_z^2)]^{1/2}\csc Z, \end{aligned} \tag{11}$$

$$\begin{aligned} C &= (E-m_z)(E'^2 - m_2^2)^{1/2} + (E'-m_2)\\ &\quad \times [(E^2 - m_y^2 - m_z^2)^{1/2} + \mathrm{i}m_y], \end{aligned} \tag{12}$$

and

$$\begin{aligned} D &= (E'^2 - m_2^2)^{1/2}[(E^2 - m_y^2 - m_z^2)^{1/2} + \mathrm{i}m_y]\\ &\quad + (E'-m_2)(E-m_z). \end{aligned} \tag{13}$$

Furthermore, the transversal wave vector k_y is set to be zero near the neutral point, while the longitudinal wave vector k_x (as shown in Eqs. (1)–(13)) is a continuum parameter due to the translation symmetry. Therefore, the system momentum averaged transmission probability is

$$T = |t|^2. \tag{14}$$

Firstly, as demonstrated in Figs. 2–4, we investigate the influence of an arbitrarily polarized ferromagnetic insulator, i.e., FM1, on the system transport properties. The influence of the polarization direction θ on the system transmission probability is presented in Fig. 2. To the best of our knowledge,[26,39,44] the z component of the exchange field should induce a gap between the conduction band and valence band, i.e., $\pm E$ for $\theta = 0$ and π while the energy band is gapless in the range of $x > 0$. Therefore, the system transmission probability T is suppressed to be nearly 0 due to the mismatch between the wave functions and the size of Fermi-surface.[26] On the other hand, the wave functions and the size of Fermi-surface are the same on both sides of the ferromagnetic insulator for the case of $\theta = \pi/2$. A maximum transmission [see

the peaks in Fig. 2] is expected, though the transmission magnitude decreases with the increase of the planar rotation angle. It is worthwhile to point out that the obtained results are good verifications of those in Figs. 2 and 3 in Ref. [26].

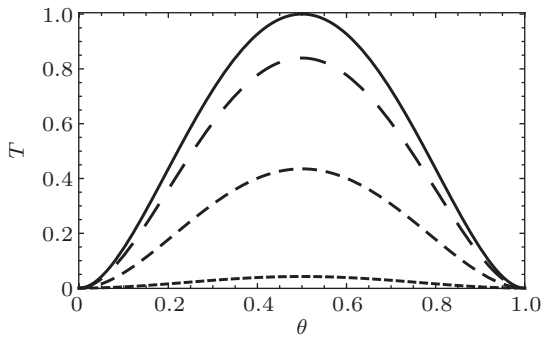


Fig. 2. Variations of single ferromagnetic insulator modulated, that is $V = m_2 = 0$, transmission probability T with polarization angle θ (in units of π) at $m_1 = E$, where the solid, dashed, short dashed, and dotted lines refer to the cases $\varphi = 0$, 0.15π, 0.30π, and 0.45π, respectively.

Furthermore, the periodical (with periodicity π and increasing amplitude with the polarization angle) dependence of the transmission probability on the planar rotation angle φ is illustrated in Fig. 3. As expected, the system presents the strongest transmission when the exchange field acts in the x direction, i.e., in the $\varphi = 0$, π, and 2π cases. While the electron transmission of the system is blockaded completely as $\varphi = \pi/2$ and $3\pi/2$, namely the exchange field points to the y axis, owing to the reduced overlapping of the k_y between the ferromagnetic insulator and surface states.[26]

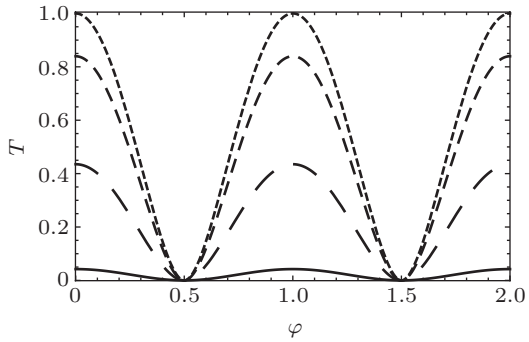


Fig. 3. Variations of transmission probability T with planar rotation angle φ (in units of π) at $m_1 = E$, where the solid, dashed, short dashed, and dotted lines refer to the cases $\theta = 0.05\pi$, 0.20π, 0.35π, and $\pi/2$, respectively.

On the other hand, the effect of ferromagnetic proximity exchange field strength m_1 on the transmission probability is shown in Fig. 4. Since the energy gap between the conduction band and valence band increases with m_1 in the range of $0 \leq \theta < \pi/2$, the transmission probability decreases with the increase of m_1, and the role played by $m_z = m_1 \cos\theta$ tends to vanish with the increasing of the polarization angle θ. However, one may expect a strengthened role played by m_z in the range of $\pi/2 < \theta \leq \pi$ [not shown here]. In all, the system transmission probabilities are sensitively dependent on the polarization direction and strength of the magnetization,[26–28,39,40,44–46] owing to the variations of the Fermi-surface and wave functions matching conditions.

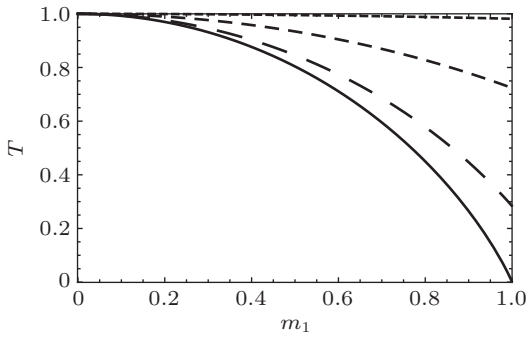


Fig. 4. Variations of transmission probability T with ferromagnetic exchange strength m_1 (in units of E) at $\varphi = 0$, where the solid, dashed, short dashed, and dotted lines refer to the cases $\theta = 0$, 0.15π, 0.30π, and 0.45π, respectively.

Since the Dirac electrons can be tuned into being n-type electron-like and p-type hole-like when the potential drop V contained in the interface between the left ferromagnetic insulator and the right ferromagnetic insulator is modulated (by the gate voltage) to be lower and higher than Fermi energy E_F, respectively, we investigate the transmission probabilities for n–n junction with $V = 0.5E_F$ and n–p junction with $V = 1.5E_F$ in Figs. 5–7. The transmission probability T as a function of polarization angle θ (in units of π) for n–n junction and n–p junction is plotted in Figs. 5(a) and 5(b), respectively. As demonstrated by the solid, dashed, and short dashed lines in Fig. 5(a) for the $Z = 0.05$, 0.20, and 0.35 cases respectively, the transmission probability first increases and then decreases with the increase of the polarization angle, while it is steadily increasing for the $Z = 0.50$ case as illustrated by the dotted line in Fig. 5(a). Owing to the combined modulations of the double ferromagnetic insulators and the interface potential, the system transmission is not symmetrically[26] distributed around $\theta = \pi/2$ as the single barrier case in Fig. 2. Furthermore, one obtains a large magnetoresistance[20–22] in the presence of an n–n junction, since the transmission probabilities for parallelly (namely $\theta = 0$) and antiparallelly ($\theta = \pi$) aligned ferromagnetic insulators are much different. It is noted that the sensitive dependence of the transmission on barrier strength Z is due to the rotation of the spin of the Dirac electron through the barrier region. However, the situation for n–p junction is somewhat different. As shown by the solid and dotted lines in Fig. 5(b) for $Z = 0.05$ and 0.50 cases, the probabilities are steadily increasing and decreasing, respectively, while they first decrease and then increase for the $Z = 0.20$ and 0.35 cases [with lower oscillation amplitude than that in the n–n junction case] as demonstrated by the dashed and short dashed lines in Fig. 5(b). It is worthwhile to point out that the results here are qualitatively consistent with those in Figs. 2(b) and 2(d) in Ref. [26],

and one expects a contrary magnetoresistance in the presence of the n–p junction to the n–n junction.

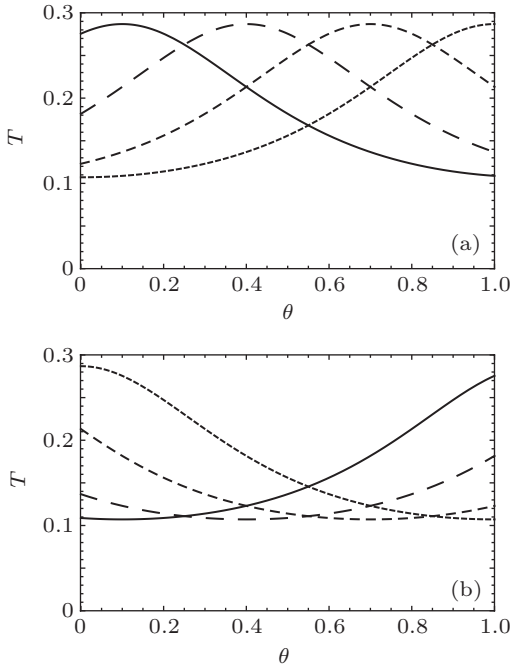


Fig. 5. Variations of double ferromagnetic insulators modulated transmission probability T with θ (in units of π) for (a) n–n junction with $V = 0.5E_{\rm F}$, and (b) n–p junction with $V = 1.5E_{\rm F}$, respectively, with $\varphi = \pi/2$, $m_1 = 0.95E$, and $m_2 = 0.30E$. The solid, dashed, short dashed, and dotted lines refer to the cases $Z = 0.05$, 0.20, 0.35, and 0.50, respectively.

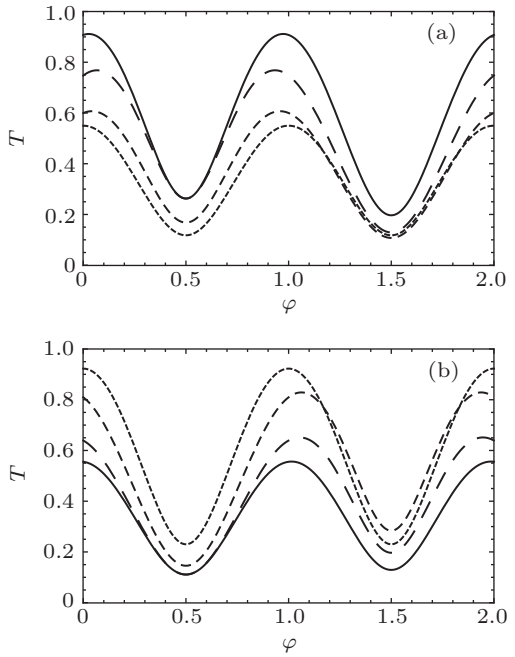


Fig. 6. Variations of transmission probability T with φ (in units of π) for (a) n–n junction and (b) n–p junction, respectively, with $\theta = \pi/4$, $m_1 = 0.95E$, and $m_2 = 0.30E$. The solid, dashed, short dashed, and dotted lines refer to the cases $Z = 0.05$, 0.20, 0.35, and 0.50, respectively.

Furthermore, the transmission probabilities as a function of in-plane rotation angle φ (in units of π) for the n–n junction and the n–p junction are illustrated in Figs. 6(a) and 6(b), respectively. The interface potentials and the actions of the much different polarized double ferromagnetic insulators suppress the geometrical symmetry and wave vector distribution of the proposed device. Therefore, the system transmission probability is not a periodical function of the planar angle φ any more, except for the transmission probabilities represented by the dotted line in Fig. 6(a) for the $Z = 0.50$ case and by the solid line in Fig. 6(b) for the $Z = 0.05$ case. Moreover, the smallest transmission probabilities at $\varphi = \pi/2$ and $3\pi/2$ decrease and increase with the increase of the barrier strength for the n–n junction and the n–p junction, respectively, while the strongest transmissions are shifted away from $\varphi = 0$, π, and 2π [see the peaks in Figs. 6(a) and 6(b)].

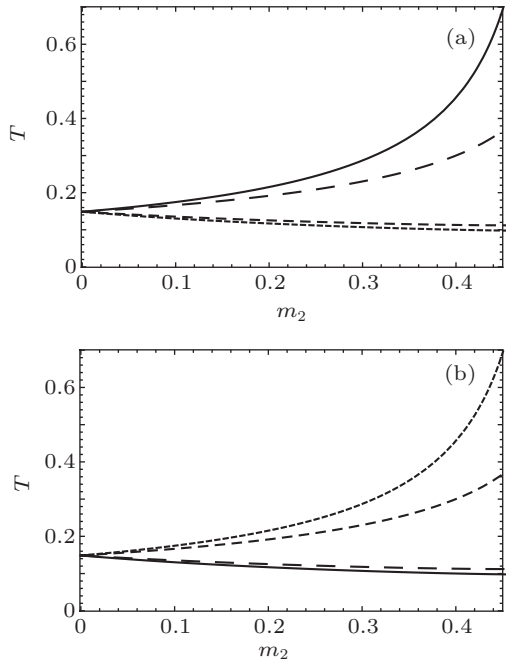


Fig. 7. Variations of transmission probability T with m_2 (in units of E) for (a) n–n junction and (b) n–p junction, respectively, while the φ, m_1, and Z are fixed at $\pi/2$, $0.95E$, and 0. The solid, dashed, short dashed, and dotted lines refer to the cases $\theta = 0$, $\pi/4$, $3\pi/4$, and π, respectively.

Finally, the dependences of transmission probability on exchange field m_2 (in units of E) for the n–n junction and the n–p junction are demonstrated in Figs. 7(a) and 7(b), respectively. Since the energy gap between the conduction band and valence band first narrows and then widens in the ranges of $0 \leq \theta < \pi/2$ and $\pi/2 < \theta \leq \pi$, the system transmission probability increases rapidly and then decreases slowly with the increase of m_2, as shown by the lines in Fig. 7(a). Unlike the case of the n–n junction, the transmission probability for the n–p junction decreases slowly for the case of $0 \leq \theta < \pi/2$ and increases fast in the range $\pi/2 < \theta \leq \pi$ with the increase of m_2 as demonstrated by the lines in Fig. 7(b). Physically,[26,39,43–46] the opposite variation trend between the n–n and n–p junctions should be understood in the following. The transmission probability for the n–n junction is determined by the overlapping of the same eigenfunctions while

that for the n–p junction is contributed from the different eigenfunctions.

In the above description, we have theoretically investigated the transport properties for the surface state Dirac electrons of a topological insulator under the modulation of a 2D ferromagnet/ferromagnet junction at the clean limit and low temperatures. The transmission probability modulated by the single ferromagnetic barrier is observed to oscillate periodically with the polarization angle and planar rotation angle, and decreases with the strength of the magnetic proximity exchange increasing. However, owing to the combined effects of the double ferromagnetic insulators and the barrier potential, the transmission probabilities for the n–n junction and the n–p junction are not a periodic function of the polarization angle nor planar rotation angle. Following the narrowed and widened energy gaps between the conduction band and valence band, the transmission probability of the n–n junction first increases rapidly and then decreases slowly in the ranges $0 \leq \theta < \pi/2$ and $\pi/2 < \theta \leq \pi$, respectively, while that of the n–p junction presents actually the opposite variation trend with the increase of the strength of the magnetic proximity exchange. The novel transmission features of the Dirac electrons on the surface of topological insulators may shed light on the realization of a magnetic/electric switch[40] based on topological insulators, and the further understanding of the surface states[47–52] of topological insulators.

References

[1] Qi X L and Zhang S C 2007 *Rev. Mod. Phys.* **83** 1057
[2] König M, Wiedmann S, Brüne C, Roth A, Buhmann H, Molenkamp L W, Qi X L and Zhang S C 2007 *Science* **318** 766
[3] Yu R, Zhang W, Zhang H J, Zhang S C, Dai X and Fang Z 2010 *Science* **329** 61
[4] Yu R, Fang Z and Dai X 2011 *Physics* **40** 462 (in Chinese)
[5] Jiang H, Chen S G, Sun Q F and Xie X C 2011 *Physics* **40** 454 (in Chinese)
[6] Cheng P, Zhang T, He K, Chen X, Ma X C and Xue Q K 2011 *Physics* **40** 449 (in Chinese)
[7] Ye F and Su G 2010 *Physics* **39** 564 (in Chinese)
[8] Wang H C and Wang J 2012 *Physics* **41** 705 (in Chinese)
[9] Chen Y L, Analytis J G, Chu J H, Liu Z K, Mo S K, Qi X L, Zhang H J, Lu D H, Dai X, Fang Z, Zhang S C, Fisher I R, Hussain Z and Shen Z X 2009 *Science* **325** 178
[10] Yuan J H, Cheng Z, Zhang J J, Zeng Q J and Zhang J P 2012 *Chin. Phys. B* **21** 047203
[11] Wu K H and Li Y Q 2011 *Physics* **40** 440 (in Chinese)
[12] Chang K 2011 *Physics* **40** 458 (in Chinese)
[13] Noh H J, Koh H, Oh S J, Park J H, Kim H D, Rameau J D, Valla T, Kidd T E, Johnson P D, Hu Y and Li Q 2008 *Europhys. Lett.* **81** 57006
[14] Hsieh D, Xia Y, Qian D, Wray L, Meier F, Dil J H, Osterwalder J, Patthey L, Fedorov A V, Lin H, Bansil A, Grauer D, Hor Y S, Cava R J and Hasan M Z 2009 *Phys. Rev. Lett.* **103** 146401
[15] Li H C, Sheng L, Sheng D N and Xing D Y 2010 *Phys. Rev. B* **82** 165104
[16] Zhang T, Cheng P, Chen X, Jia J F, Ma X C, He K, Wang L L, Zhang H J, Dai X, Fang Z, Xie X C and Xue Q K 2009 *Phys. Rev. Lett.* **103** 266803
[17] Hsieh D, Xia Y, Wray L, Qian D, Pal A, Dil J H, Osterwalder J, Meier F, Bihlmayer G, Kane C L, Hor Y S, Cava R J and Hasan M Z 2009 *Science* **323** 919
[18] Roth A, Brüne C, Buhmann H, Molenkamp L W, Maciejko J, Qi X L and Zhang S C 2009 *Science* **325** 294
[19] San J P, Prada E, McCann E and Schomerus H 2009 *Phys. Rev. Lett.* **102** 247204
[20] Burkov A A and Hawthorn D G 2010 *Phys. Rev. Lett.* **105** 066802
[21] Soodchomshom B 2010 *Phys. Lett. A* **374** 2894
[22] Kong B D, Semenov Y G, Krowne C M and Kim K W 2011 *Appl. Phys. Lett.* **98** 243112
[23] Gao J H, Yuan J, Chen W Q, Zhou Y and Zhang F C 2011 *Phys. Rev. Lett.* **106** 057205
[24] Mahfouzi F, Nikolić B K, Chen S H and Chang C R 2010 *Phys. Rev. B* **82** 195440
[25] Semenov Y G, Duan X P and Kim K W 2012 *Phys. Rev. B* **86** 161406
[26] Yokoyama T, Tanaka Y and Nagaosa N 2010 *Phys. Rev. B* **81** 121401
[27] Zhang K H, Wang Z C, Zheng Q R and Su G 2012 *Phys. Rev. B* **86** 174416
[28] Gao J H, Chen W Q, Feng X Y, Xie X C and Zhang F C 2009 arXiv: 0909. 0378v1
[29] Ma X H, Ma P, Jiao Y, Yang L Y, Ma J G, He Q, Jiao S S, Zhang J C and Hao Y 2011 *Chin. Phys. B* **20** 097302
[30] Huang W, Wang Z L and Yan M L 2010 *Chin. Phys. Lett.* **27** 067304
[31] Cao J X, Yan X H, Xiao Y and Ding J W 2003 *Chin. Phys.* **12** 1440
[32] Chen Q, Li T C, Shi Q W and Wang X P 2005 *Acta Phys. Sin.* **54** 3962 (in Chinese)
[33] Zeng H, Hu H F, Wei J W, Xie F and Peng P 2006 *Acta Phys. Sin.* **55** 4822 (in Chinese)
[34] Chen J W and Yang L F 2005 *Acta Phys. Sin.* **54** 2183 (in Chinese)
[35] Guo W, Hu Y B, Zhang Y Y, Du S X and Gao H J 2009 *Chin. Phys. B* **18** 2502
[36] Chen F, Chen Y P, Zhang M and Zhong J X 2010 *Chin. Phys. B* **19** 086105
[37] Chen L N, Ma S S, Ouyang F P, Wu X Z, Xiao J and Xu H 2010 *Chin. Phys. B* **19** 097301
[38] Mondal S, Sen D, Sengupta K and Shankar R 2010 *Phys. Rev. Lett.* **104** 046403
[39] Ueda H T, Takeuchi A, Tatara G and Yokoyama T 2012 *Phys. Rev. B* **85** 115110
[40] Linder J, Tanaka Y, Yokoyama T, Sudb A and Nagaosa N 2010 *Phys. Rev. B* **81** 184525
[41] Zhai F and Mu P Y 2011 *Appl. Phys. Lett.* **98** 022107
[42] Wang H Y, Chen X W, Zhou X Y, Zhang L B and Zhou G H 2012 *Physica B* **407** 3364
[43] Zhang Y and Zhai F 2010 *Appl. Phys. Lett.* **96** 172109
[44] Alos P M, Tiwari R P and Blaauboer M 2012 *New. J. Phys.* **14** 113003
[45] Zhang J P and Yuan J H 2012 *Eur. Phys. J. B* **85** 100
[46] Yuan J H, Zhang Y, Zhang J J and Cheng Z 2013 *Eur. Phys. J. B* **86** 36
[47] Wu Z H, Peeters F M and Chang K 2010 *Phys. Rev. B* **82** 115211
[48] Wu Z H, Peeters F M and Chang K 2011 *Appl. Phys. Lett.* **98** 162101
[49] Wickles C and Belzig W 2012 *Phys. Rev. B* **86** 035151
[50] Shao H H, Zhou X Y, Li Y, Liu G H and Zhou G H 2011 *Appl. Phys. Lett.* **99** 153104
[51] Zhou X Y, Shao H H, Liu Y M, Tang D S and Zhou G H 2012 *J. Phys.: Condens. Matter* **24** 185301
[52] Zhao L, Liu J W, Tang P Z and Duan W H 2012 *Appl. Phys. Lett.* **100** 131602